Published in final edited form as:
Chem Commun (Camb). 2017 May 04; 53(37): 5227–5230. doi:10.1039/c7cc01620d.

[FeFe] Hydrogenase Active Site Model Chemistry in a UiO-66 Metal-Organic Framework

Sonja Pullen[a], **Souvik Roy**[a], and **Sascha Ott**[*,a]

[a]Department of Chemistry, Ångström Laboratory, Uppsala University, Box 523, 75120 Uppsala, Sweden

Abstract

The reactivity of $[Fe_2(dcbdt)(CO)_6]$ (**1**) confined in a UiO-66(Zr) metal-organic framework towards CO ligand substitutions with phosphines of different sizes was investigated. The reaction with smaller phosphines (PX_3, X = Me, Et) is more selective compared to analogous reactions in homogenous solution phase, and two CO ligands at up to 80% of all [FeFe] sites in UiO-66-**1** are replaced. The produced $[Fe_2(dcbdt)(CO)_4(PX_3)_2]$ complexes in the UiO-66 matrix behave like typical [FeFe] hydrogenase active site model complexes, are reduced at more cathodic potentials than their hexacarbonyl analogues, and form bridging hydrides under acidic conditions.

Metal-organic frameworks (MOFs) possess well-defined porous structures with high internal surface areas, as well as great flexibility in design.1, 2 As such, they provide appealing platforms for the incorporation of molecular organometallic catalysts.3–5 Functionality can be introduced into the organic linker molecules either directly during solvothermal synthesis of the framework,6 while thermally unstable or reactive functional groups can be installed post-synthetically through post-synthetic modifications (PSM)7 or post-synthetic linker exchange (PSE).2, 8 The combination of organometallic catalysts and MOFs is motivated for mainly two reasons: catalyst immobilization often leads to improved structural stability of the catalyst and thus higher turnover numbers, while remaining organic linkers in the MOF may carry further functional groups that can interact favourably with the incorporated catalysts. Such higher coordination sphere effects would be reminiscent to the situation in enzymes,9, 10 and may include for example hydrogen-bonding or steric interactions that fine-tune the electronics of the incorporated catalysts.

We have recently reported the introduction of a dinuclear iron complex $[Fe_2(dcbdt)(CO)_6]$ (**1**, dcbdt = 1,4-dicarboxylbenzene-2,3-dithiolate) with structural features of the [FeFe] hydrogenase (H_2ase) active site11, 12 into a UiO-66(Zr) (UiO = University of Oslo)13 MOF under mild PSE conditions.14 Owing to the stabilizing effect of the UiO-66,15 the resulting UiO-66-**1** is a superior proton reduction catalyst compared to the homogenous reference system.14, 16

The set of six CO ligands in UiO-66-**1** is different to that in the H_2ase active site where two electron donating cyanides are found in addition to the CO ligands.11 The purpose of these

sascha.ott@kemi.uu.se.

ligands has been modelled in [FeFe] H_2ase active site mimics where substitution of CO ligands by similarly stronger donor ligands like phosphines is a popular strategy to increase the basicity of the metal centres,17 and thus to enable the formation of hydrides without the need for prior electrochemical reductions.12, 18 With the favourable properties that are provided by the UiO-66 framework, we were intrigued whether CO ligands in UiO-66-**1** could be replaced by electron donating phosphines also within the pores of a MOF (Figure 1).

In general, ligand exchange at organometallic linkers inside MOF cavities is challenging because the incoming ligand has to migrate over 100s of nanometers through the entire MOF crystal to reach complexes that are localized deeply inside the porous material. In addition, the incoming phosphine ligands that were used in this study (Figure 1) are all larger than the initially present CO ligands, thus potentially leading to steric congestions that may prevent high yielding CO→phosphine ligand exchanges.

Lastly, a specific complication in the case of **1** with its bdt-derived ligand is that its exposure to phosphines in homogenous solution leads to two major products: the desired twofold ligand-exchanged $[Fe_2(bdt)(CO)_6(PX_3)_2]$ (bdt = benzene-1,2-dithiol, X = Me, Et or Ph) alongside the formation of a mononuclear Fe(II) complex of the general formula $[Fe(bdt)(CO)_2(PX_3)_2]$. The question thus arises whether the reactivity of **1** is altered by the surrounding MOF matrix, and whether a different product distribution can be obtained as a function of MOF incorporation.

UiO-66-**1** with a loading of approx. 14% of **1** was prepared by PSE as reported earlier (see ESI, Fig. S1).14 Its average crystal dimension is circa 800 nm (ESI, Fig. S2) with octahedral and tetrahedral pores of an average window size of 6 Å.13 The FT-IR spectrum of UiO-66-**1** is characterized by ν_{CO} stretching frequencies at 2073, 2038 and 1997 cm^{-1} that arise from the [FeFe] complex (Figure 2). Three different phosphines PX_3 (X = Me, Et, Ph) were used for the ligand exchange experiments, with PMe_3 and PEt_3 being smaller than the average UiO-66 pore window, while PPh_3 is bigger (Figure 1).

Molecular references were obtained for bdt instead of dcbdt complexes due to the ready availability of the former and their generally good solubility. The impact of bdt *vs.* dcbdt ligand on the electronic properties of the Fe_2 complexes is comparable as exemplified by almost identical FT-IR spectra (Table 1). $[Fe_2(bdt)(CO)_4(PX_3)_2]$ were obtained from $[Fe_2(bdt)(CO)_6]$ by a room temperature protocol using Me_3NO as a decarbonylation agent. 19 The reaction of $[Fe_2(bdt)(CO)_6]$ with the phosphines results in the formation of two products, roughly in a 2:1 ratio. As exemplified for PMe_3, the major product is the dincuclear, disubstituted complex $[Fe_2(bdt)(CO)_4(PMe_3)_2]$, while the minor one is the mononuclear $[Fe(bdt)(CO)_2(PMe_3)_2]$.20 Similar reactivity has also been observed for the reaction of $[Fe_2(bdt)(CO)_6]$ with cyanide.16

Ligand exchange on UiO-66-**1** was performed by stirring a suspension of the former with an excess of Me_3NO and the phosphine at ambient temperature for up to 5 days. Importantly, the crystallinity of the UiO-66 under the ligand exchange conditions is preserved even on the timescales of days, as evidenced by PXRD and SEM (see ESI, Fig. S2 & S3). For UiO-66-**1**

treated with PMe_3, the best results were obtained after stirring for 24 hours when approximately 80 % of the complexes have converted to a new species as demonstrated by FT-IR spectroscopy. This new species is characterized by ν_{CO} frequencies at 1980, 1942, 1911 cm^{-1} (Fig. 2 and Table 1), and is assigned to UiO-66-incorporated $[Fe_2(dcbdt)(CO)_4(PMe_3)_2]$ on grounds of its IR spectrum that is very similar to that of the homogenous $[Fe_2(bdt)(CO)_4(PMe_3)_2]$ reference (Table 1). The small average discrepancy of circa $\Delta\nu_{CO}$ = 9 cm^{-1} for all three bands is most likely due to the difference between bdt and deprotonated, Zr-coordinated dcbdt. After 24 hours, no further exchange was observed, even after prolonged reaction times to five days and the addition of further Me_3NO and phosphine.

The incomplete transformation despite a large excess of reagents points towards a steric protection of some of the $[Fe_2(dcbdt)(CO)_6]$ sites inside the UiO-66 framework. Phosphine exchanged complexes that are formed at early stages of the experiment are most likely responsible for blocking access to some of the remaining $[Fe_2(dcbdt)(CO)_6]$ sites inside the UiO-66. It is noteworthy that the reaction of UiO-66-**1** with PMe_3 produces only one product, the UiO-66-incorporated $[Fe_2(dcbdt)(CO)_4(PMe_3)_2]$. This reactivity is different to that in homogenous phase where in addition to the PMe_3-substituted [FeFe] complex also the mononuclear $[Fe(bdt)(CO)_2(PMe_3)_2]$ is observed. It thus seems that MOF incorporation of the organometallic complex alters its reactivity. In the reported mechanism for the formation of the mononuclear species,16 the cleavage of one of the Fe-S bonds in an early intermediate is the junction point from which the two product species arise. As the thiolate is part of the dcbdt ligand that is integral to the UiO-66 framework, it may be that this Fe-S cleavage is sterically disfavored, thus preventing the formation of the mononuclear product. Also, an intermediate with two bdt ligands that is postulated at a later stage of $[Fe(bdt)(CO)_2(PMe_3)_2]$ formation would not be attainable for the UiO-66 confined [FeFe] complex.

The reaction of UiO-66-**1** with PEt_3 shows a similar ligand exchange behavior as that of PMe_3, and UiO-66-incorporated $[Fe_2(dcbdt)(CO)_4(PEt_3)_2]$ is observed by its ν_{CO} bands at 1983, 1945 and 1918 cm^{-1} after 24 hours (Figure 2 and Table 1) as the only product. The ligand exchange yield for the PEt_3 substitution reaction is circa 50%, and thus lower than that in the PMe_3 case. This difference is most likely an effect of the larger size of the PEt_3 ligands that, when coordinated to the Fe_2 complex, more efficiently block the UiO-66 pores. For the largest ligand PPh_3, no significant ligand exchange is observed, even after 5 days reaction of UiO-66-**1** with excess amounts of both Me_3NO and ligand (see ESI). The lack of reactivity in case of PPh_3 demonstrates that the ligand exchange reactions are true PSMs, and do not proceed through metallolinkers that transiently have leached into solution phase.

Introduction of phosphine ligands leads to an increased electron density at the iron centers, as indicated by a shift to lower ν_{CO} stretching frequencies. Such a higher electron density will push the reduction potential of the complexes cathodically; an effect that was probed by cyclic voltammetry (CV, see ESI for details). As UiO-type MOFs are intrinsically non-conducting,21, 22 only redox active species that reside at the periphery of the MOF crystals are electrochemically accessible. CVs with acceptable current responses can be obtained by contacting the crystals to the glassy carbon working electrode through carbon black (see ESI for details).23 As illustrated in Figure 3a, the CV of UiO-66-**1** displays a partially reversible redox process at a formal $E_{1/2}$ = –1.05 V ($E_{p,c}$ = –1.18 V and $E_{p,a}$ = –0.91 V). This wave is

assigned to $[Fe_2(dcbdt)(CO)_6]$ inside the UiO-66-**1** on grounds of its similarity to reported solution values.24 The CV of the framework after treatment with PMe_3 (Fig. 3b) features an irreversible reduction at –2.05 V in addition to the process at –1.05 V. This wave can be attributed to the disubstituted $[FeFe](dcbdt)(CO)_4(PMe_3)_2$ based on an earlier report of analogous complexes.20 As expected, the feature at –2.05 V is gradually lost over consecutive scans, an observation which is consistent with the irreversible nature of this redox process. As only Fe_2 complexes at the periphery of the MOF crystal can be addressed electrochemically, the detection of unsubstituted $[Fe_2(dcbdt)(CO)_6]$ in the CV in Figure 3b is somewhat surprising, and suggests that not only Fe_2 sites deeply buried in the MOF crystal are protected from ligand substitution, but also some that are near the crystal surface.

As mentioned above, the introduction of phosphine ligands increases the electron density at the Fe_2 sites and potentially allows the formation of hydride species which are prominent intermediates in the catalytic proton reduction cycle. Thus, the reactivity of UiO-66-incorporated $[Fe_2(dcbdt)(CO)_4(PMe_3)_2]$ towards triflic acid was investigated. While the 800 nm sized UiO-66 samples gave inconclusive results, protonation of $[Fe_2(dcbdt)(CO)_4(PMe_3)_2]$ in smaller crystals of 300 nm could unambiguously be observed by FT-IR spectroscopy (see Fig. 4 and ESI). Starting from a UiO-66 sample with circa 80% of the Fe_2 sites being $[Fe_2(dcbdt)(CO)_4(PMe_3)_2]$, conversion to a new species that is characterized by two strong absorptions at ν_{CO} = 2054 and 2016 cm^{-1} can be detected. These absorptions are very similar to those of related $[Fe_2(adt)(CO)_4(\mu\text{-}H)(PMe_3)_2]$25 (adt = azadithiolate) and $[Fe_2(pdt)(CO)_4(\mu\text{-}H)(PMe_3)_2]$26 (pdt = propyldithiolate) that carry bridging hydride ligands, and the species that is produced within the UiO-66 framework is thus assigned to the UiO-66-$[Fe_2(dcbdt)(CO)_4(\mu\text{-}H)(PMe_3)_2]$. Notably, the crystallinity of the framework remains unchanged after treatment with triflic acid as indicated by PXRD (ESI, Fig. S6). Quantitative formation of the hydride species occurs on the timescale of minutes, pointing towards cumbersome access into the material.27 As the hydride species are intermediates in catalytic proton reduction schemes, their slow formation is a critical aspect that needs to be taken into account, for example when devising future electrocatalytic materials.

In conclusion, we have shown that CO→phosphine ligand substitutions are possible inside MOFs as long as the introduced ligands can enter the pore windows. Using an excess of phosphine ligand and Me_3NO allowed 50-80% conversion of $[Fe_2(dcbdt)(CO)_6]$ into the dinuclear disubstituted complexes as the only products. The reactivity of $[Fe_2(dcbdt)(CO)_6]$ is thus altered by its confinement in the UiO-66, and mononuclear side products that are observed in homogenous phase are absent in the MOF. UiO-66-$[Fe_2(dcbdt)(CO)_4(PMe_3)_2]$ can be protonated to form the hydride species UiO-66-$[Fe_2(dcbdt)(CO)_4(\mu\text{-}H)(PMe_3)_2]$ which is a prominent intermediate during catalytic proton reduction cycles.

Supplementary Material

Refer to Web version on PubMed Central for supplementary material.

Acknowledgments

Financial support for this work was provided by the Swedish Research Council, the Swedish Energy Agency, the Wenner-Gren Foundations (postdoctoral stipend to S. R.), and the European Research Council (ERC-

CoG2015-681895_MOFcat). Mrs. Ashleigh Castner is acknowledged for her contributions to the synthetic part of the paper.

Notes and references

1. Burnett BJ, Barron PM, Hu C, Choe W. J Am Chem Soc. 2011; 133:9984–9987. [PubMed: 21671680]
2. Yoon M, Srirambalaji R, Kim K. Chem Rev. 2012; 112:1196–1231. [PubMed: 22084838]
3. Evans JD, Sumby CJ, Doonan CJ. Chem Soc Rev. 2014; 43:5933–5951. [PubMed: 24736674]
4. Wang J-L, Wang C, Lin W. ACS Catalysis. 2012; 2:2630–2640.
5. Liu J, Chen L, Cui H, Zhang J, Zhang L, Su CY. Chem Soc Rev. 2014; 43:6011–6061. [PubMed: 24871268]
6. Wang C, Xie Z, deKrafft KE, Lin W. J Am Chem Soc. 2011; 133:13445–13454. [PubMed: 21780787]
7. Cohen SM. Chem Rev. 2012; 112:970–1000. [PubMed: 21916418]
8. Cohen SM. J Am Chem Soc. 2017; doi: 10.1021/jacs.6b11259
9. Zhang M, Gu Z-Y, Bosch M, Perry Z, Zhou H-C. Coordination Chemistry Reviews. 2015; 293–294:327–356.
10. Cohen SM, Zhang Z, Boissonnault JA. Inorg Chem. 2016; 55:7281–7290. [PubMed: 27231968]
11. Lubitz W, Ogata H, Rudiger O, Reijerse E. Chem Rev. 2014; 114:4081–4148. [PubMed: 24655035]
12. Li Y, Rauchfuss TB. Chem Rev. 2016; 116:7043–7077. [PubMed: 27258046]
13. Valenzano L, Civalleri B, Chavan S, Bordiga S, Nilsen MH, Jakobsen S, Lillerud KP, Lamberti C. Chem Mater. 2011; 23:1700–1718.
14. Pullen S, Fei H, Orthaber A, Cohen SM, Ott S. J Am Chem Soc. 2013; 135:16997–17003. [PubMed: 24116734]
15. Burtch NC, Jasuja H, Walton KS. Chem Rev. 2014; 114:10575–10612. [PubMed: 25264821]
16. Streich D, Karnahl M, Astuti Y, Cady CW, Hammarström L, Lomoth R, Ott S. Eur J Inorg Chem. 2011; 2011:1106–1111.
17. Vlugt JIvdRauchfuss TB, Wilson SR. Chem Eur J. 2006; 12:90–98.
18. Tard C, Pickett CJ. Chem Rev. 2009; 109:2245–2274. [PubMed: 19438209]
19. Gloaguen F, Lawrence JD, Schmidt M, Wilson SR, Rauchfuss TB. J Am Chem Soc. 2001; 123:12518–12527. [PubMed: 11741415]
20. Schwartz L, Singh PS, Eriksson L, Lomoth R, Ott S. Comptes Rendus Chimie. 2008; 11:875–889.
21. Hendon CH, Tiana D, Walsh A. PCCP. 2012; 14:13120–13132. [PubMed: 22858739]
22. Lin S, Pineda-Galvan Y, Maza WA, Epley CC, Zhu J, Kessinger MC, Pushkar Y, Morris AJ. ChemSusChem. 2016; 10:514–522. [PubMed: 27976525]
23. Mijangos E, Roy S, Pullen S, Lomoth R, Ott S. Dalton Trans. 2017; 46:4907–4911. [PubMed: 28345708]
24. Fei H, Pullen S, Wagner A, Ott S, Cohen SM. Chem Commun. 2015; 51:66–69.
25. Schwartz L, Eilers G, Eriksson L, Gogoll A, Lomoth R, Ott S. Chem Commun. 2006:520–522.
26. Zhao X, Georgakaki IP, Miller ML, Yarbrough JC, Darensbourg MY. J Am Chem Soc. 2001; 123:9710–9711. [PubMed: 11572707]
27. Roy S, Pascanu V, Pullen S, González Miera G, Martín-Matute B, Ott S. Chem Commun. 2017; 53:3257–3260.

Europe PMC Funders Author Manuscripts

One sentence summary

CO→phosphine ligand exchange reactions on [FeFe(dcbdt)$(CO)_6$] incorporated in UiO-66(Zr) afford selectively the disubstituted UiO-66-[FeFe(dcbdt)$(CO)_4(PX_3)_2$] which can be protonated quantitatively to afford the bridging hydride UiO-66-[FeFe(dcbdt)(μ-H)$(CO)_4(PX_3)_2$].

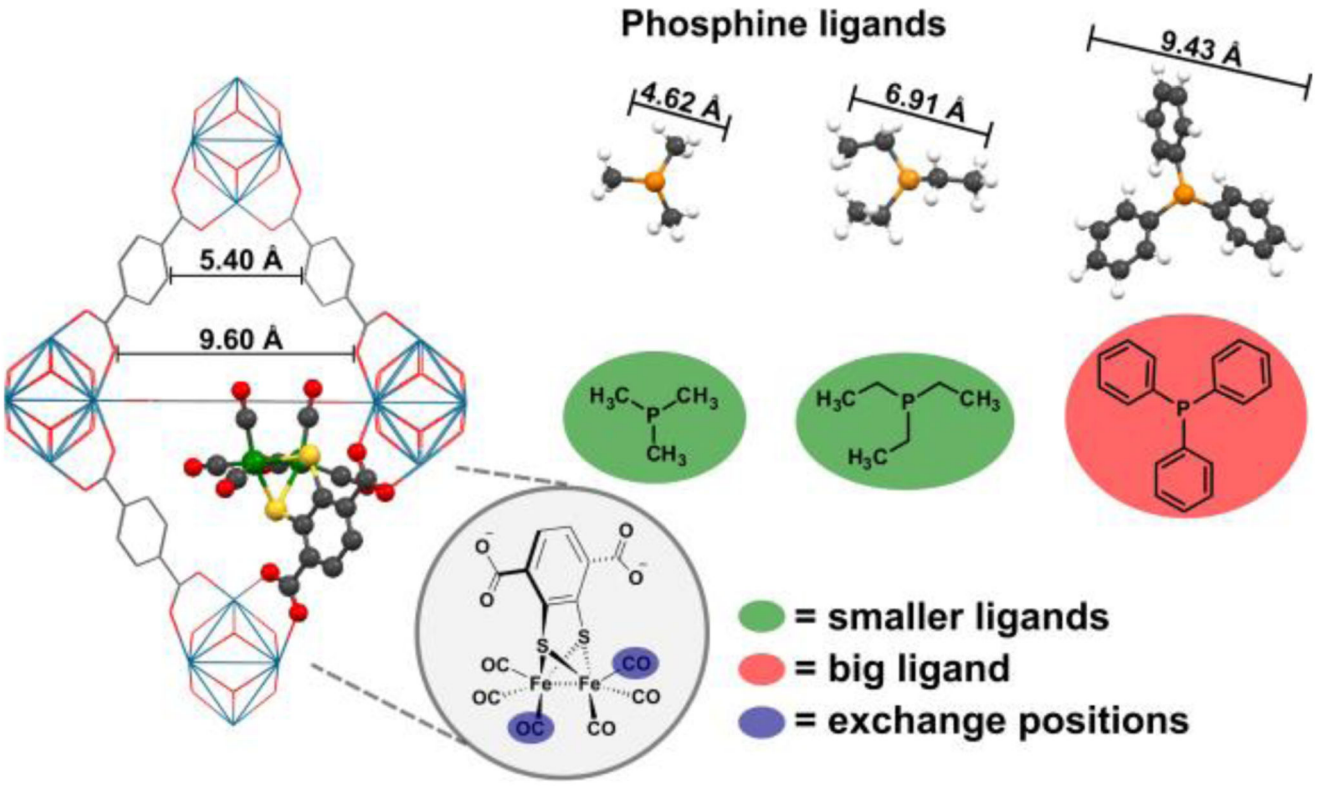

Figure 1.

Schematic presentation of CO→phosphine ligand exchange reactions in UiO-66-[Fe_2(dcbdt)$(CO)_6$] using PMe_3, PEt_3 and PPh_3.

Europe PMC Funders Author Manuscripts

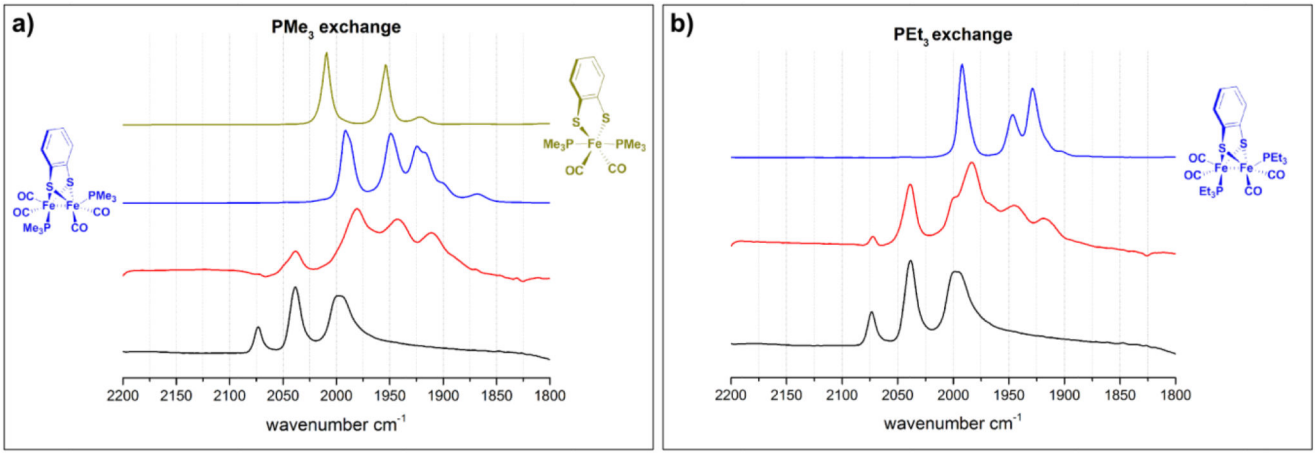

Figure 2.

IR spectra of ligand exchange reactions in UiO-66-**1** before (black) and after (red) addition of PMe_3 a) and PEt_3 b). Reference complexes [FeFe](bdt)$(CO)_4(PX_3)_2$ (X = Me or Et) in blue and [Fe](bdt)$(CO)_2(PMe_3)_2$ in gold. All spectra were recorded in CH_3CN solutions/ suspensions.

Europe PMC Funders Author Manuscripts

Europe PMC Funders Author Manuscripts

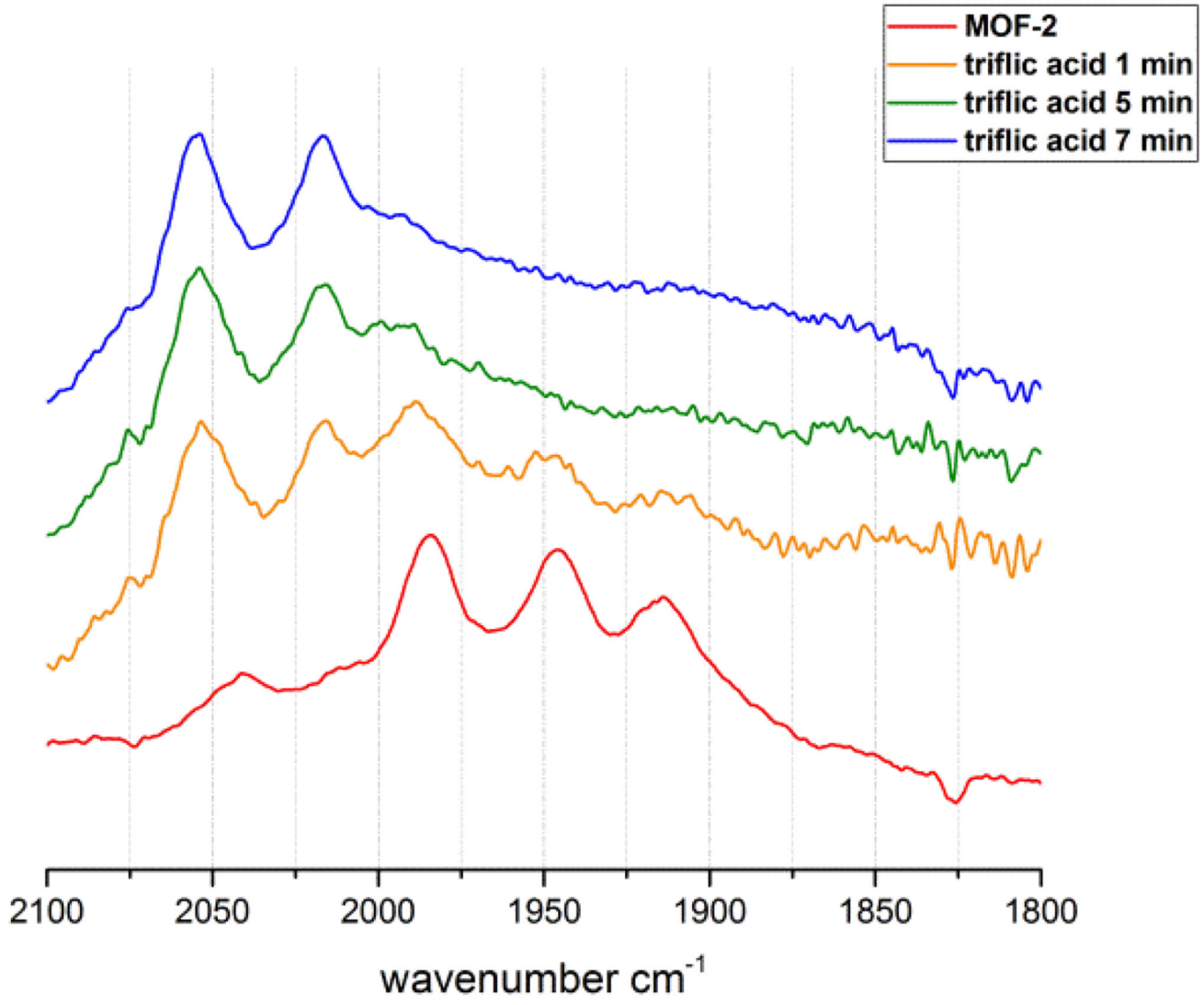

Figure 3.

Protonation of UiO-66-**2**. Yellow to blue: 1 mg UiO-66-**2** was added to a solution of triflic acid (11.3 mM in CH_3CN); IR spectra of the suspension were recorded in a liquid IR cell. In red: reference spectrum of UiO-66-**2** in pure CH_3CN.

Europe PMC Funders Author Manuscripts

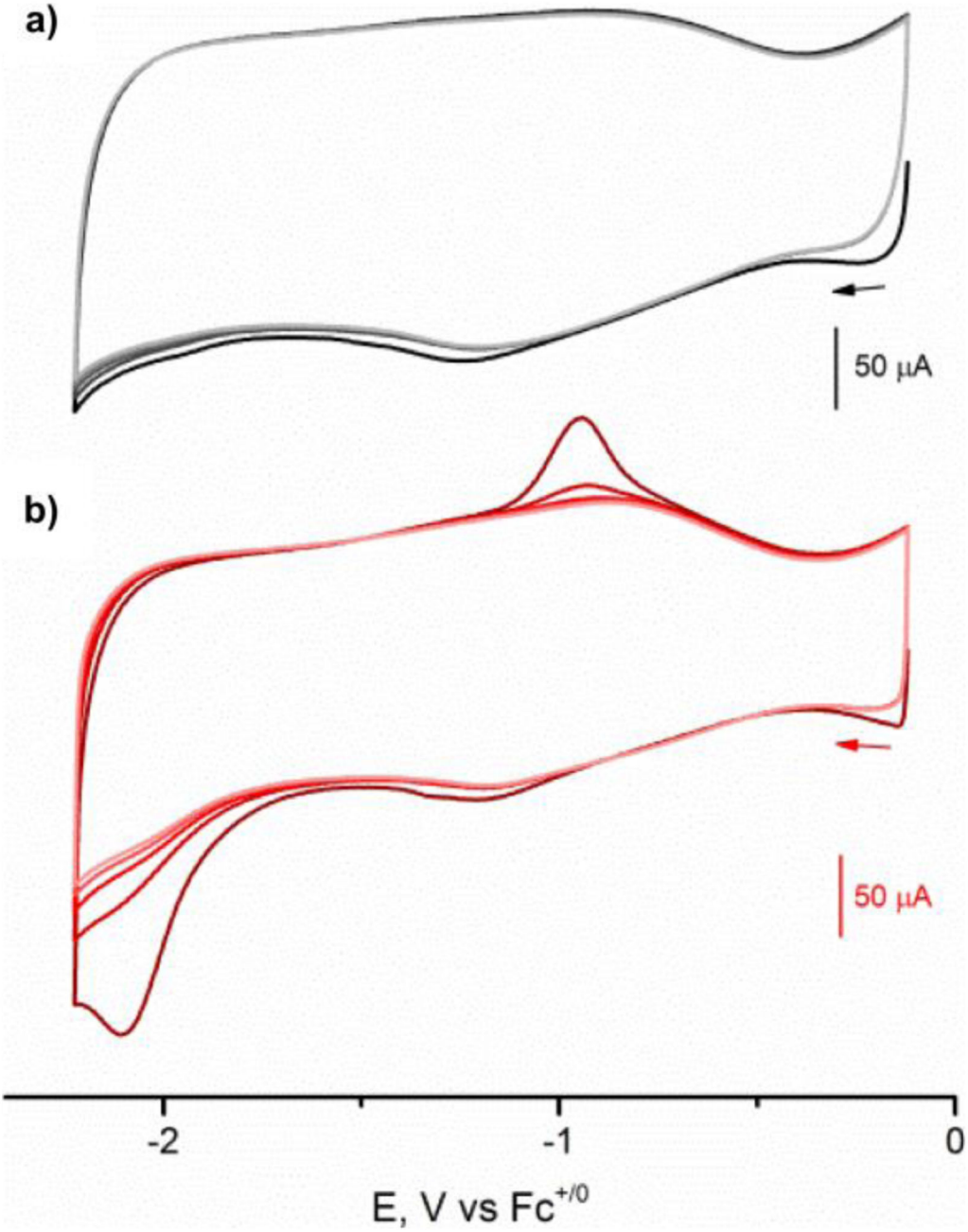

Figure 4.

Progressive cyclic voltammograms of a) UiO-66-**1** and b) UiO-66-**2** modified glassy carbon electrodes. Voltammograms were recorded in acetonitrile containing 0.1 M NBu_4PF_6 at 100 mV s^{-1}; first five scans are presented in each case.

Europe PMC Funders Author Manuscripts

Table 1

IR frequencies for all reference complexes and MOFs.

Material	IR frequencies (ν_{CO} in cm^{-1})
UiO-66-**1**	2073, 2038, 1997
$[Fe_2(dcbdt)(CO)_6$ (**1**)	2082, 2046, 2007
$[Fe_2(bdt)(CO)_6]$	2078, 2042, 2002
UiO-66-$[Fe_2(dcbdt)(CO)_4(PMe_3)_2]$	1980, 1942, 1911 *1)*
difference spectrum (see Fig S4a)	1985, 1946, 1916
$[FeFe](bdt)(CO)_4(PMe_3)_2$	1991, 1948, 1924
$[Fe](bdt)(CO)_2(PMe_3)_2$	2009, 1954
UiO-66-$[Fe_2(dcbdt)(CO)_4(PEt_3)_2]$	1983, 1945, 1918 *1)*
difference spectrum (see Fig S4b)	1982, 1944, 1917
$[FeFe](bdt)(CO)_4(PEt_3)_2$	1992, 1947, 1929
$[FeFe](bdt)(CO)_4(PPh_3)_2$	2001, 1957, 1941

*1*Given are the prominent absorptions associated with the ligand-substituted $[FeFe](dcbdt)(CO)_4(PX_3)_2$ in the UiO-66. All FT-IR spectra were recorded in CH_3CN solution/suspension.